Proceeding of the Third International & the Fifth Scientific Conference of College of Science - Tikrit University
Int.3, Loc.5, Article ID:2022-P3-15

Purposeful scientific research is a basic pillar for the advancement of Iraq

The effect of irradiation by gamma ray on the structural and optical properties of nickel oxide nanoparticles prepared by sol-gel method.

S. A. Mohammed , J. Al-Zanganawee, O. A. Muwaffaq
Department of Physics, College of Science, University of Diyala, Iraq
Jasimmansoor13@gmail.com , Alzanganawee@uodiyala.edu.iq

ABSTRACT
In this work. NiO, NPs were synthesized using the Sol-Gel technique at various molar ratios of nickel nitrate and citric acid (P_1, P_2 and P_3) and annealed at 525°C, and study the effect of irradiation on the structural and optical properties of nickel oxide nanoparticles. According to the XRD data, every sample is polycrystalline, with a cubic structure as its preferred orientation (200) plane, And that these results largely agree with the standard card (ICSD No. 047-1049). And when comparing the behavior of the grains before and after irradiation, we notice that there is an increase in the intensity of the diffraction peaks for all prepared samples compared to what it was before irradiation. The results showed that the grain size was less than it was before the irradiation, and this means that the irradiation caused an increase in the crystallization of the grains and thus a decrease in the size of the crystals. (FESEM) images of nickel oxide nanoparticles before and after irradiation showed that irradiation reduces the size of the granules except for the sample (P_3), which shows the opposite and these results. The optical results showed that the gamma ray irradiation process led to a slight increase in the absorbance and absorption coefficient, as well as a decrease in the optical energy gap.

Keywords: Nickel oxide nanoparticles, Sol- Gel, FESEM, Optical Measurements and Radiation

Introduction
NiO, one of several nanostructured metal oxides, has caught the interest of scientists and researchers due to its fundamental scientific applications. Nickel (II) oxide is one of the few transition metal oxides with a tendency to be p-type, and it shows a lot of promise as a candidate for use in optical amplifiers, tunable lasers, magnetic materials, catalytic materials, sensitive materials for chemoresistive or optical gas sensors, and other applications[1]. The creation of the NiO NPs manufacturing process has required a lot of effort[2]. Although it is still in its early stages, research on the synthesis of nanostructured nickel oxide has primarily concentrated powder, solution, and thin films[3]. Sol-gel, microwave plasma, co-precipitation, and hydrothermal are just a few of the processes that can be used to create NiO nanoparticles[4,5]. The aim of this research is to use the sol-gel method to prepare NiO nanoparticles and study the effect of irradiation on the structural and optical properties of nickel oxide nanoparticles.

2. Experimental details
The nickel oxide nanoparticle (NiO NPs) was prepared by Sol- Gel method at various molar ratios of nickel nitrate and citric acid (P_1, P_2 and P_3) by dissolving Nickel(II) nitrate hexahydrate $Ni(NO_3)_2.6H_2O$ in (100 ml) of distilled water at a concentration (0.3M), and dissolving citric acid ($C_6H_8O_7.H_2O$) in (50 ml) drops by drops of the mixture. Ammonium hydroxide (NH4OH, Merck) was added until solutions reached pH 5.5. The solutions were well mixed by magnetic stirrer and setting the temperature at 75 ^oC, gel was formed, and then dry it in the oven for (10 h). Table (1), represents the weights and molarity used to prepare the nickel oxide nanoparticles. Then the resulting powder is calcined at (525 °C,) for three hours. The Gamma Chamber 900 system, located at the University of Baghdad - College of Science - Department of Physics Was used in the process of irradiating samples of pure (p_1, p_2 and p_3) nickel oxide nanoparticles at a temperature (525 ^oC), where this system contains the source cobalt-60 (Co60) manufactured by the Bhabha Atomic Research Center of India (BARC). Topography of the surface of the films was imaged using FESEM (MIRA3, TE-SCAN). The structural properties are used X-ray diffraction (Shimadzu XRD/6000) was used With a wavelength (λ=1.54060Å) and optical properties (Shimadzu, UV- 1800) in the wavelength range of (300 – 900) nm.

Table 1: Represents the weights and molarity used to prepare the nickel oxide nanoparticles

Sample	Mass of Nickel nitrate g	Volume of Distilled Water mL	Molar of Nickel nitrate M	Mass of Citric Acid g	Volume of Distilled Water mL	Molar of Citric Acid M	The molar ratio between nickel nitrate and citric acid
P_1	**8.72439**	**100**	**0.3**	**4.72819**	**50**	**0.45**	**1.33-1**
P_2	**8.72439**	**100**	**0.3**	**3.15219**	**50**	**0.3**	**2-1**
P_3	**8.72439**	**100**	**0.3**	**2.10149**	**50**	**0.2**	**3-1**

3- Results and discussions

(3-1) Results of XRD

The X-ray diffraction results of pure nickel oxide (NiO) (P_1, P_2 and P_3) granules prepared at a temperature of (525 °C) before and after gamma ray irradiation are shown in Figure (1), and the diffraction results of NiO and Ni nanoparticles are shown. It is of a polycrystalline structure and of a cubic type. Figure (1) shows the X-ray diffraction patterns for all samples prepared before and after the irradiation process. We note that in NiO powder appears in (2θ ~ 37.3°, 43.4°, 63°, 75.5° and 79.5°) corresponding to the levels (111), (200), (220), (311) and (222), respectively, and that the prevailing trend of growth (200) and there is no change in the prevailing trend before and after irradiation [6], and these results are very much in agreement with the international card with serial number (ICDD 047-1049) of NiO, and we note that in Ni powder appears in (2θ ~ 44.507°, and 51.846 79.5°) corresponding to the levels (111), (200) respectively, and these results are agreement with the card number (ICDD 040-850) of Ni, and the results of (XRD) are shown in general that there was no change in the type of composition and the prevailing trend of all the prepared granules, and that they behave the same as the granules before irradiation in terms of increasing the intensity, but when comparing the behavior of the granules.

Before and after irradiation, we notice that there is an increase in the intensity of the diffraction peaks for all the prepared samples compared to what it was before irradiation, and that the increase in intensity is accompanied by an increase in the mid-top width (FWHM) as shown in Figure (1) with a decrease in the value of the crystal size, There is also a creep towards a decrease in the diffraction angles, which could be the reason for the changes taking place in an improvement in the crystallization of the grains as a result of irradiation for all grains compared to their values before irradiation, because irradiation leads to changes in the structural structure of the grains [7].

The distance between crystalline levels (d(hkl) was calculated for all the samples prepared using Bragg's Law according to the relation (1) before and after irradiation with gamma rays and as shown in Table 2 . Through Table we notice that there is a very slight change in the values of (d) for the particles before irradiation compared with the particles after irradiation, This confirms that irradiation has an effect on the crystal structure of the prepared granules[7].

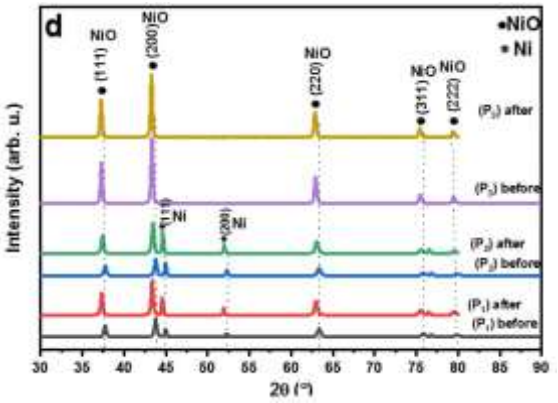

Fig. 1: X-ray diffraction of Ni and NiO grains before and after irradiation.

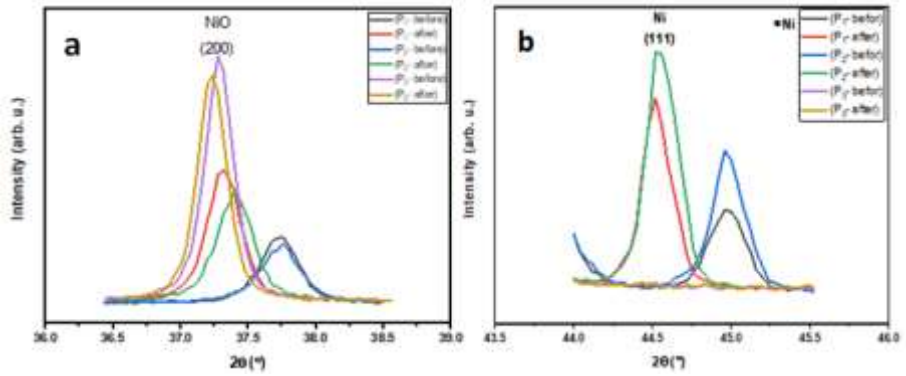

Fig. 2: X-ray diffraction of (a) NiO grains to the dominant direction (200) and (b) Ni to the dominant direction (111) before and after irradiation.

$$n\lambda = 2 d_{hkl} \sin\theta_B \ldots\ldots (1)$$

where, d_{hkl}: The distance between interplanar spacing, θ_B: Brack angle, λ: (wavelength, n: an integer called the order of reflection.

Table 2: Diffraction angles, Miller's coefficients, interlayer distances and (FWHM of the as-prepared nanoparticles.

Sample Code	2θ (^{o})	(hkl)	d_{hkl} (Å)	FWHM (^{o})
P_1- before	44.8884	(200)	2.0176	0.2443
P_1- after	43.3653	(200)	2.0849	0.2837
P_2- before	44.9281	(200)	2.0159	0.2311
P_2- after	43.4411	(200)	2.0814	0.3032
P_3- before	43.3593	(200)	2.0852	0.1938
P_3- after	43.2792	(200)	2.0889	0.2460

The lattice constant (a_o) was calculated from the X-ray diffraction patterns according to the relationship (2) for all grains prepared before and after gamma-ray irradiation. The reason is due to the increase in crystallization of the grains as we mentioned previously, as shown in Table (3), and it is also possible that a disturbance occurred in the crystal lattice as a result of irradiation [8].

$$\mathbf{d_{hkl}} = \frac{a_o}{\sqrt{h^2+k^2+l^2}} \quad \text{..... (2)}$$

The crystalline size (D_{av}) of all prepared granules was calculated using the Scherrer formula (3) and Williamson-Hall formula(4), before and after irradiation for the dominant plane (200). It is clear from the results that the average particle size has decreased from what it was before irradiation, as noted from table (3), and this means that irradiation caused an increase in the crystallization of the granules and thus a decrease in the size of crystals [9]. The decrease in the size of the crystals is an indication of the improvement of the crystallization and quality of the material [10]. Figure (3) show the relation between the variables through which the crystal size was calculated according to (Williamson-Hall) method for nickel oxide before and after irradiation. Figure (4) show the relation between (D_{222}) and (β_{222}) as a function of doping ratios of non-irradiated, irradiated and annealed NiO grains at a temperature of (525 ^{o}C).

$D_{av} = K\lambda / \beta \cos\Theta_B$.....(3)

where, K constant = (0.9), λ: the wavelength of the X-rays falling on the target. β: Full Width at Half Maximum (FWHM) measured in radial units.

$$\beta_{hkl}\cos\theta = \left(\frac{K\lambda}{D}\right) + 4S\sin\theta \quad \text{.....(4)}$$

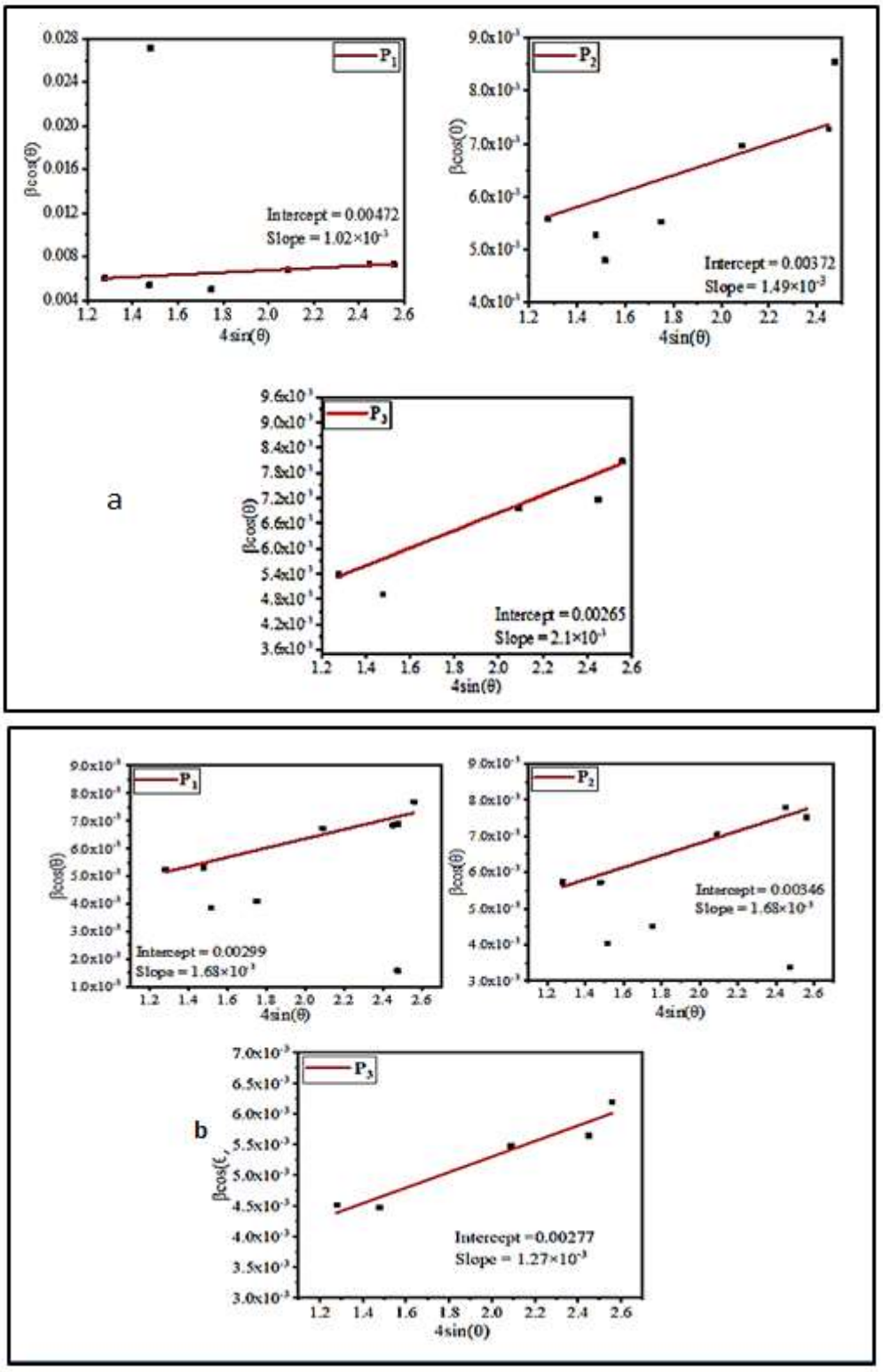

Fig. 3: The relationship between the variables through which the crystal size was calculated according to (Williamson-Hall) method for nickel oxide grains NiO: (a) before irradiation (b) after irradiation.

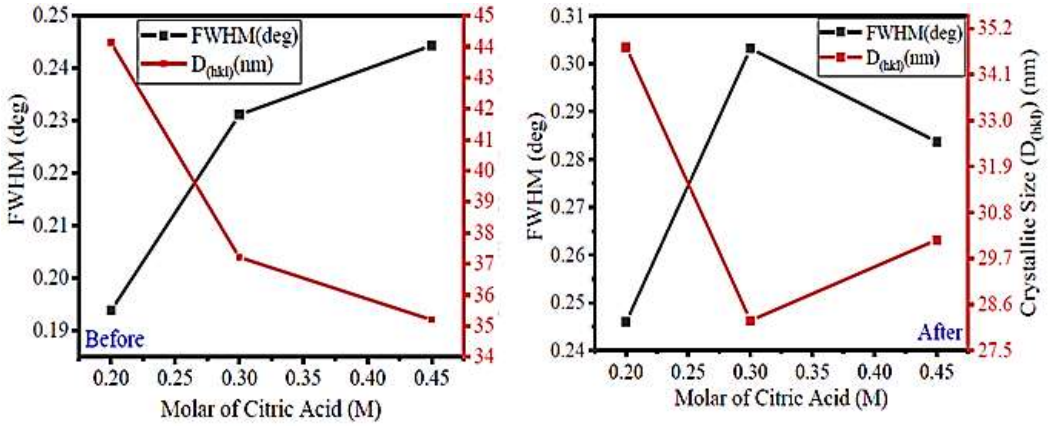

Fig. 4: The relationship between (D_{222}) and (β_{222}) as a function of doping ratios of non-irradiated, irradiated and annealed NiO grains at a temperature of (525 oC).

(Tc) for all prepared granules was calculated using the relationship (4), which describes the dominant level (hkl) for crystal growth in polycrystalline granules. Table (3) shows the values of the formation factor for all samples prepared before and after the irradiation process, where it was found that forming factor values are greater than one for pure grains before and after irradiation, and this means that the crystal direction (200) is the dominant direction and thus no change occurred in the dominant direction of grain growth[8, 10].

$$T_c = \frac{I_{(hkl)}/I_{o(hkl)}}{N^{-1}\sum_N I_{(hkl)}/I_{o(hkl)}} \quad \ldots\ldots \quad (4)$$

where :

I_o (hkl): represents the standard intensity of the level (hkl) of the standard card.

N: represents the number of peaks visible in X-ray diffraction (XRD).

I (hkl): represents the measured relative intensity of the level (hkl).

5. Dislocation Density (δ)

The values of dislocation intensity (δ) were calculated using the relationships (5), for all pellets prepared before and after irradiation[9].

$$\delta = \frac{1}{D^2} \quad \ldots.(5)$$

Table (3) shows the values of (δ) for all samples prepared before and after irradiation. When comparing the values after irradiation, we notice an increase in the values of the intensity of dislocations compared to their values before irradiation for all samples prepared due to the decrease in the size of the crystals as a result of irradiation because the intensity of dislocations are inversely proportional to the average crystal size according to the relationships (5), and as shown in table (3). These results indicate an improvement in the growth and crystallization of the prepared material as a result of irradiation with gamma rays because irradiation may increase or decrease defects [10].

Table 3: some parameters obtained from X-ray diffraction results.

Sample Code	2θ (°)	(hkl)	T_C	$\varepsilon \times 10^{-4}$	$\delta \times 10^{-4}$ (nm)$^{-2}$	Crystallite Size (D_{hkl}) (nm)	
						Scherrer	W.H
P_1- before	44.8884	(200)	1.1905	9.84797	8.07181	35.1977	33.756
P_1- after	43.3653	(200)	1.1751	11.49793	11.00315	30.1468	28.12
P_2- before	44.9281	(200)	1.4286	9.31453	7.22104	37.2135	38.928
P_2- after	43.4411	(200)	1.1120	12.285	12.56112	28.2154	49.462
P_3- before	43.3593	(200)	1.3158	7.85458	5.1348	44.1304	53.436
P_3- after	43.2792	(200)	1.1921	9.97298	8.27804	34.7565	38.723

(FTIR) measurements were carried out for pure and annealed nickel oxide grains at a temperature of (525 °C) before and after irradiation within the measurement range (400-4000 cm^{-1}), by measuring the transmittance spectrum as a function of wave number, as shown in Figure (5), which showed some of the vibrational bonds of the prepared grains before and after irradiation, which showed a wide range of absorption peaks at (3600-3000 cm^{-1}) representing the extended vibrations of the (O-H) bonds of the prepared samples. A strong bond of the (H-O-H) bond was observed at (1600 cm-1, and the absorption peaks were shown in the wave number between (400-500 cm^{-1}) and it was found that there was a stretching vibration in NiO)), and these results are in agreement with [11, 12], and the figures show the presence of displacement in all peaks resulting from irradiation with gamma rays, and the intensity and width of the peaks increase approximately after irradiation, except for the sample (P_2), where the intensity and width of the peaks decrease as in Figure (4). The pictures show the effect of the irradiation process on the spectrum of absorption bands (NiO), where we notice the effect is clear through the increase in the wave number of the absorption bands bonding (NiO), and this means that the absorption bands deviate towards the low photon energies and this is due to the increase in absorption and decrease in the optical energy gap.

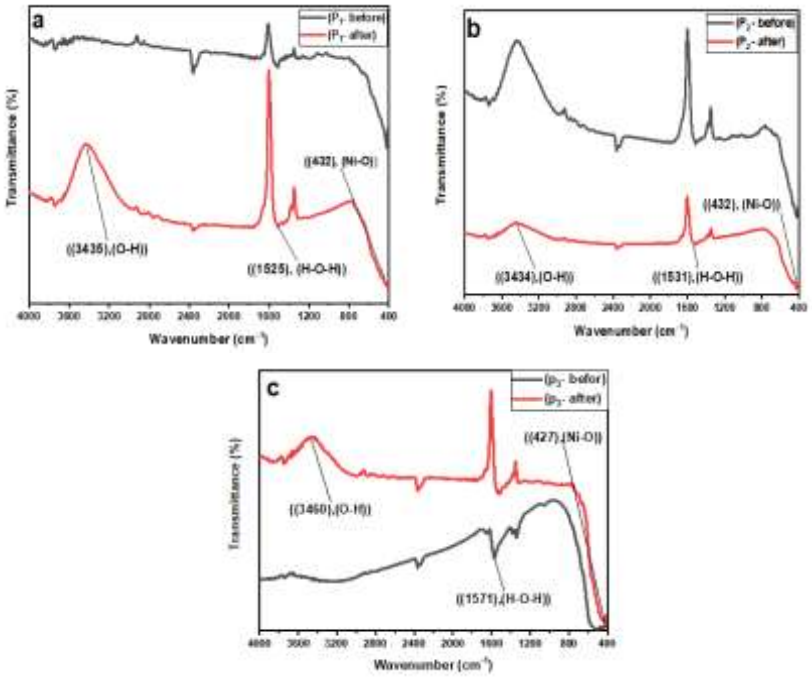

Fig. 5 a, b and c: FTIR images of Nickel oxide nanoparticles before and after irradiation

The surface morphology of the prepared granules and the extent of the effect of the irradiation process on them under the same preparation conditions followed at a temperature of (525 ºC) were studied through the field-emitting scanning electron microscope (FESEM), which can image the surface composition of the materials with very high accuracy. Figure (6) shows FESEM images of nickel oxide granules before and after irradiation. It was noted that irradiation reduces the size of the granules, except for the sample (P_3), which shows the opposite. These results are consistent with XRD assays. The images in the figures show irregular growth and distribution of oxide granules. Pure nickel prepared at a temperature of (525 °C), as it was noticed that the surface structure changed from nano-spherical granules before irradiation to spherical and other irregular shapes after irradiation with the appearance of voids and gaps clearly and that the size of the granules decreases significantly after a process[12], it is noticed from table (4) that there is a difference in the particle size due to the inhomogeneity of the prepared material well.

Table 4: average particle size values for the prepared granules.

Sample Code	P_1		P_2		P_3	
	before	after	before	after	before	after
Average Grain Size (nm)	141.4	47.7	58.2	47.8	38.9	51.2

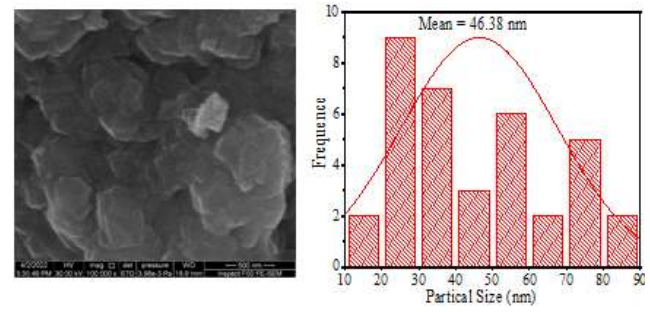

p_1 525 before

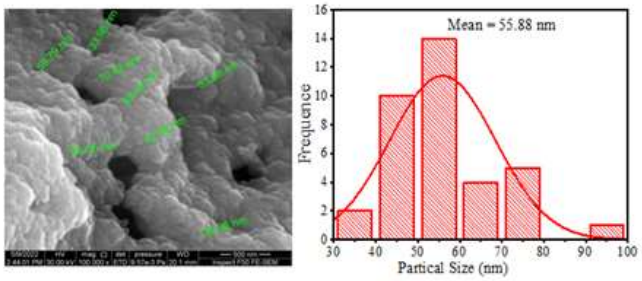

p_1 525 after

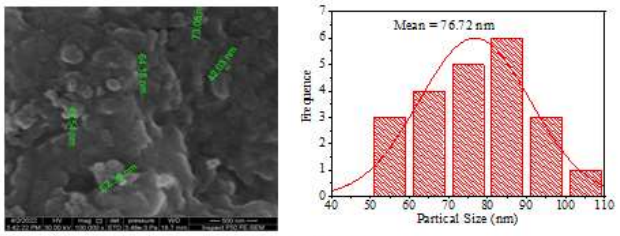

p_2 525 before

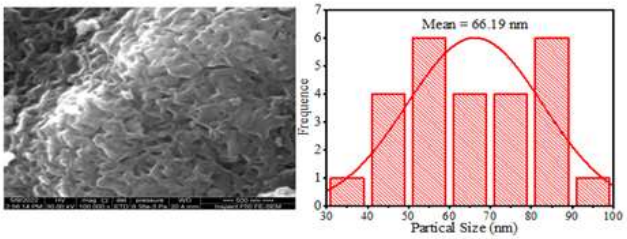

p_2 525 after

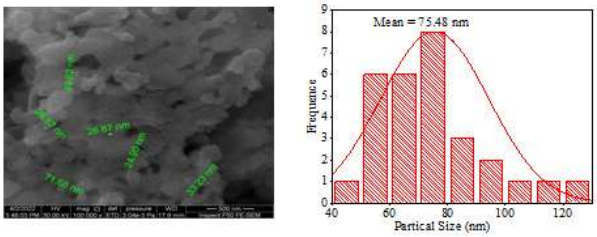

p_3 525 before

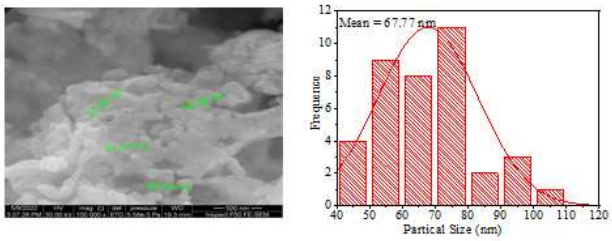

P3 525 after

Fig. 6: FESEM images of NiO grains before and after irradiation.for (P_1,P_2,P_3) respectivly

Figure (7) shows Energy Dispersive Spectroscopy (EDS), as it is an analytical method that enables us to identify the chemicals in the sample composition and know their proportions in addition to ensuring their presence. EDS analysis showed the presence of nickel and oxygen (Ni, O) in different proportions. It is noted from the results that irradiation has a clear effect through a decrease in the ratio of nickel to oxygen. During the calcination process, the carboxy group of
GO is decomposed and a large number of gases are emitted, such as CO_2, CO and H_2O.27 The contraction of d-spacing also reflects that the GO was reduced to graphene

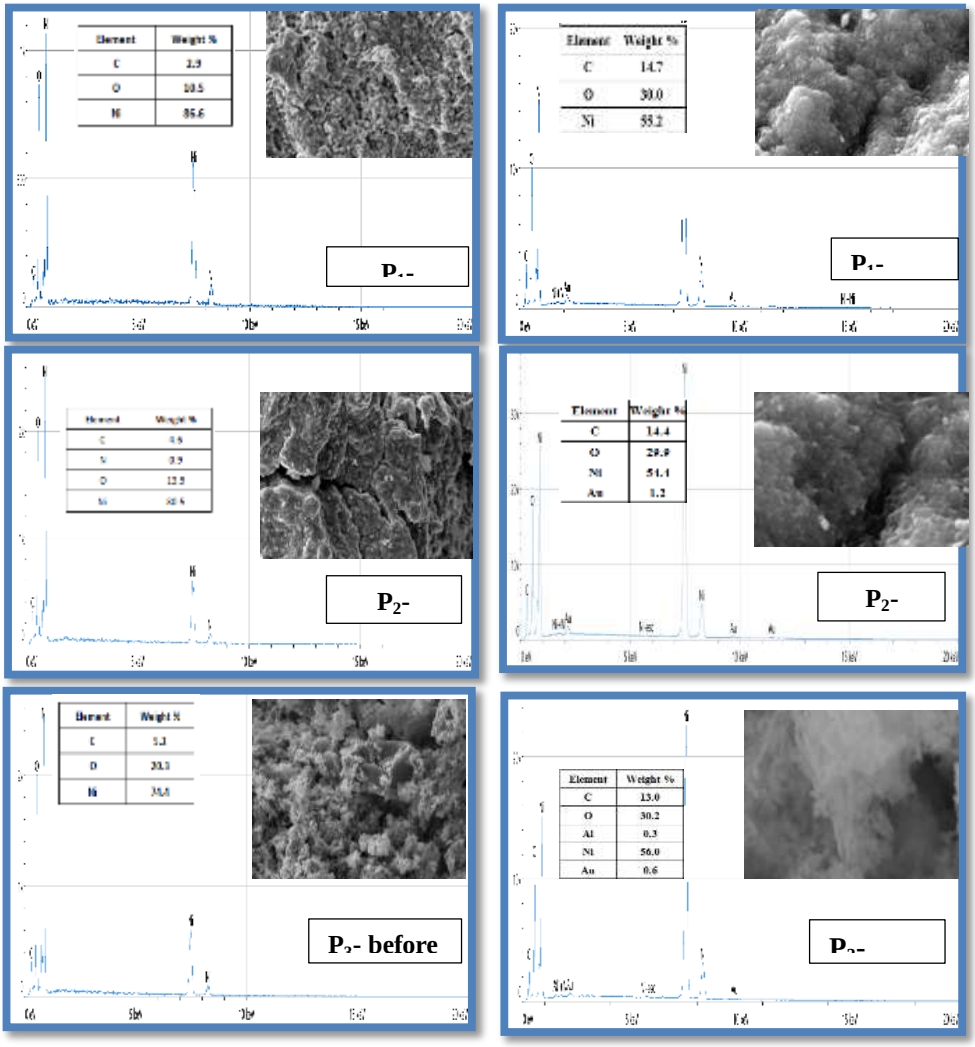

Fig. 7: EDS analyzes of nickel oxide grains before and after irradiation.

Optical properties are of great importance in studying the behavior of semiconducting optical materials, through which the appropriate practical application can be known. The optical behavior is closely related to the crystal structure of the material and the structure of energy levels. The optical properties of nickel oxide grains (P_1, P_2 and P_3) were studied, pure and annealed at a temperature (525 °C) to compare their optical properties before and after irradiation. The permissible energy gap for direct electronic transitions.

Figure (8) shows the absorbance change as a function of photon energy for pure nickel oxide granules before and after irradiation. The figure shows a decrease in the absorbance values for all samples, whether before or after irradiation as the wavelength increases, because the optical absorption spectrum values depend on both the energy of the incident photons, the type of material and its crystal structure, which leads to a decrease in the absorbance of the grains of light with the increase in the wavelength (the energy of the photon is inversely proportional to (with wavelength) and this means the lack of energy of photons needed to excite electrons and transfer them from the valence beam to the conduction beam. This is due to the fact that irradiation causes a decrease in the size of crystals as confirmed by X-ray measurements (XRD) and then a decrease in the number of localized levels within the optical energy gap, which led to a shift of the absorption edge towards high energies[13].

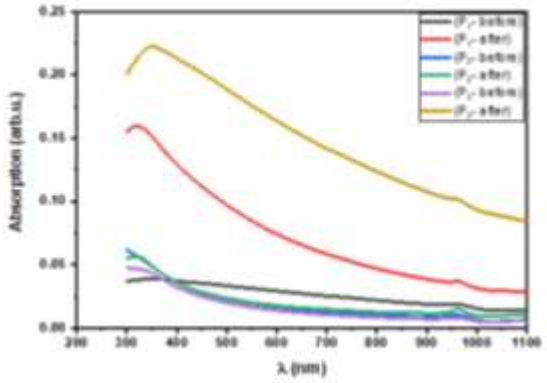

Fig. 8: Absorption spectrum of nickel oxide granules before and after irradiation.

The transmittance spectrum of pure nickel oxide grains before and after irradiation, as in Figure (9) shows an opposite behavior to the absorbance, as the transmittance for all grains is as little as possible from the basic absorption edge (short wavelengths), and the transmittance increases with increasing wavelength until Its value is established approximately after the wavelength (500 nm) in the visible spectrum region. It is also noted that the permeability spectrum of samples after irradiation is less than it was before irradiation, and it is also noted that the highest percentage of transmittance was about (95%) for sample (P_1) before irradiation, while the lowest percentage of transmittance was for sample (P_3) after irradiation. In addition, we notice from the figure a sharp rise in the transmittance, which indicates that the prepared nanoparticles have good crystallization [13]. We clearly see the effect of irradiation on nanoparticles, especially in the low region of the wavelength less than (500 nm), and this change in transmittance can be attributed to the increase in the internal energy state due to the effect of gamma rays [14].

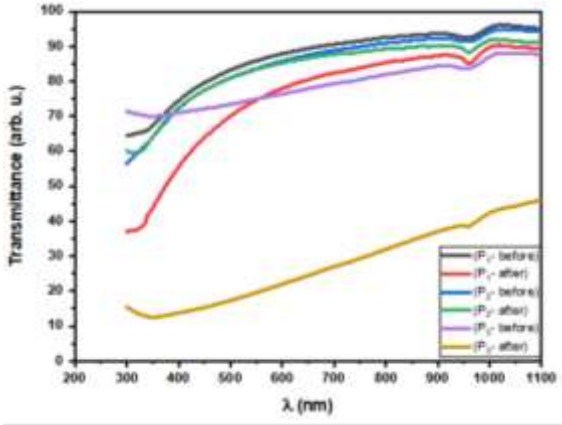

Fig. 9: Transmittance spectrum of nickel oxide granules before and after irradiation.

The absorption coefficient of all the granules before and after irradiation was calculated from the absorption spectrum of these granules, using the equation (6)[15].

$$\alpha h\nu = B_1 (h\nu - E'^{opt.}_g \pm E_{ph})^r \quad \ldots\ldots\ldots\ldots (6)$$

E'^{opt}_g : The permissible indirect transmission optical energy gap in units (eV), B_1: a constant that depends on the type of substance, E_{ph}: the energy of the auxiliary phonon in units (eV). Signal (-) means phonon absorption and sign (+) means phonon emission.

Figure (9) shows the change in the absorption coefficient (α) as a function of the energy of the nickel oxide grains before and after irradiation, and from Figure (10) We note that the grains have the same behavior as the absorption coefficient increased with the increase in the photon energy, from this increase it is possible to identify the basic absorption edge and the occurrence of transitions between the valence and conduction beams. which affected the absorption process and increased the number of electrons that could reach the conduction bundles [15]. And the high values of the absorption coefficient of the grains indicate the high probability of direct electronic transitions. [16].

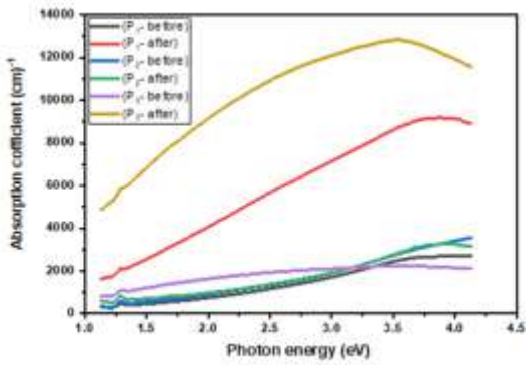

Fig. 10: absorption coefficient as a function of photon energy, For nickel oxide granules before and after irradiation.

The optical energy gap of the permissible direct electronic transitions for pure nickel oxide grains before and after irradiation was calculated as shown in Figure (10) depending on the relation (5), where the value of r = 1/2)) by drawing the linear relationship between $(\alpha h\nu)^2$ And between the energy of the incident photon (hν) shown in Figure (11) for all the prepared grains It was found that the energy gap values decrease after irradiation and this is due to an increase in the density of the states sites in the energy gap that leads to a decrease in the energy gap [16], and the table (5) shows the energy gap values (Eg) for the allowed direct transfer before and after irradiation.

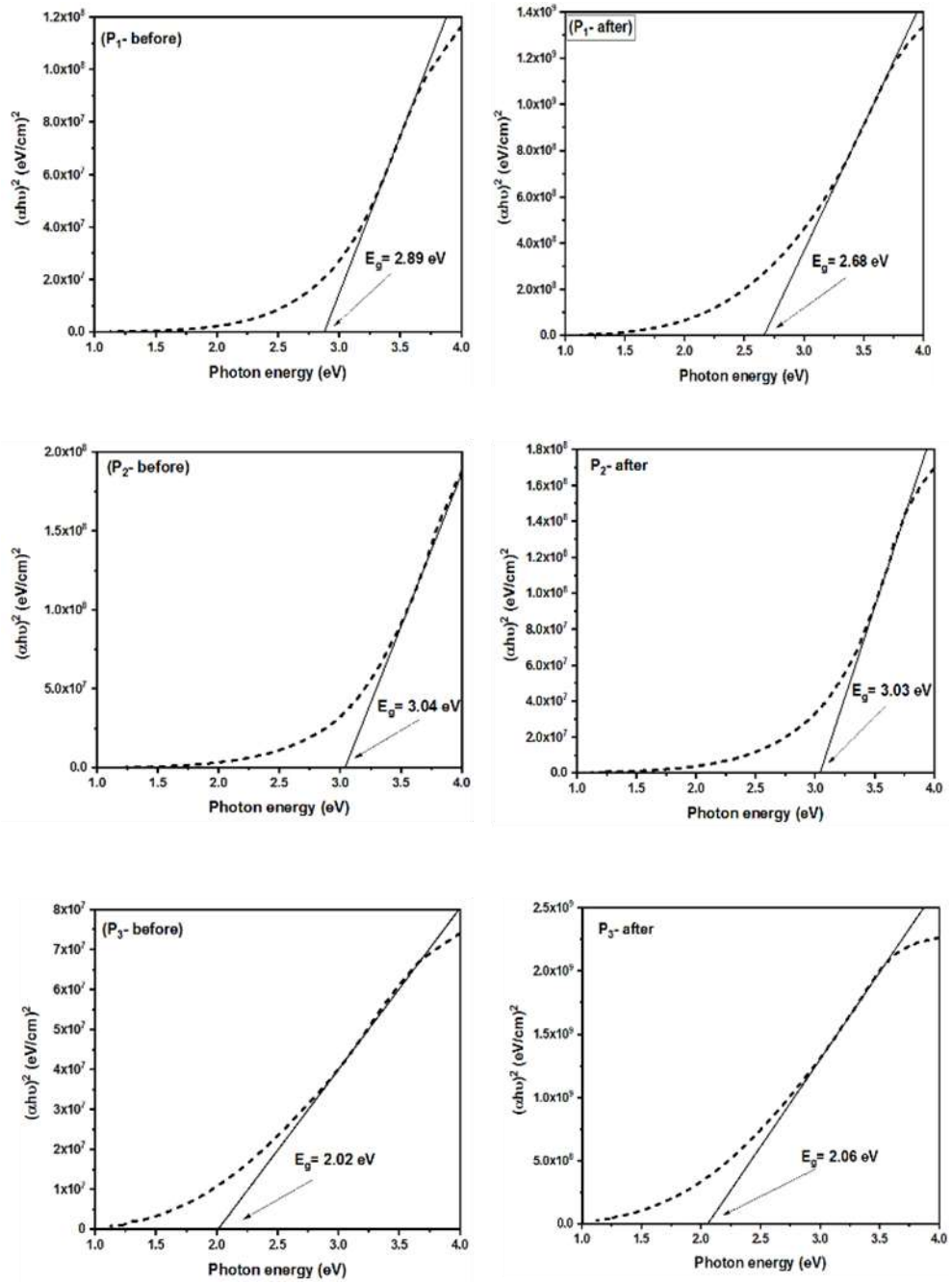

Fig. 11: Energy gap of the allowed direct transfer of nickel oxide grains before and after irradiation.

Table 5: values of the optical energy gap (Eg) for the permissible direct electronic transmission

Sample	E_g (eV) (Before radiation)	E_g (eV) (After radiation)
P_1	**2.89**	**2.68**
P_2	**3.04**	**3.03**
P_3	**2.02**	**2.06**

Conclusions

1- The possibility of preparing nickel oxide nanoparticles at a high degree using the Sol Gel Method.

2- The X-ray diagnostic results of nickel oxide granules prepared with different molar ratios before and after irradiation showed that they are of a polycrystalline structure and of a cubic type.

3. The results of FESEM indicate the growth and distribution of nickel oxide granules before and after irradiation, and that the size of the granules increased significantly with the difference in the rate of inoculation.

4- The gamma ray irradiation process led to a slight increase in the absorbance and absorption coefficient, as well as a decrease in the optical energy gap.

5. References

1. Abbas, H., Nadeem, K., Hafeez, A., Hassan, A., Saeed, N., & Krenn, H.. A, "comparative study of magnetic, photocatalytic and dielectric properties of NiO nanoparticles synthesized by sol-gel and composite hydroxide mediated method", *Ceramics International*, *45*(14), 17289-17297, (2019).
2. Huang, Y., Zhang, Y., Lin, S., Yan, L., Cao, R., Yang, R., ... & Xiang, W, "Sol-gel synthesis of NiO nanoparticles doped sodium borosilicate glass with third-order nonlinear optical properties," *Journal of Alloys and Compounds*, *686*, 564-570, (2016).
3. S. Wang, S.P. Jiang, X. Wang, "Microwave-assisted one-pot synthesis of metal/metaloxide nanoparticles on graphene and their electrochemical applications, Electrochim". Acta 56, 3338–3344, (2011).
4. B.R, S. and XR, J, "Effect of Calcination Time on Structural, Optical and Antimicrobial Properties of Nickel Oxide Nanoparticles," Journal of Theoretical and Computational Science, 03(02), (2016).
5. Ziad T. Khodair, A. A. Kamil and Y. K. Abdalaah, " Effect of annealing on structural and optical properties of Ni(1-x)MnxO nanostructures thin films ", Physica B503,55–63, (2016).
6. Adiba, Pandey, V., Munjal, S., & Ahmad, T," Structural and optical properties of sol gel synthesized NiO nanoparticles", In AIP Conference Proceedings (Vol. 2270, No. 1, p. 110011), (2020).
7. Yazdani, A., Zafarkish, H. and Rahimi, K.,"The variation of E g -shape dependence of NiO nanoparticles by the variation of annealing temperature. Materials Science in Semiconductor Processing", 74, pp.225–231, (2018).
8. Nadeem, K., Ullah, A., Mushtaq, M., Kamran, M., Hussain, S.S. and Mumtaz, M, "Effect of air annealing on structural and magnetic properties of Ni/NiO nanoparticles," Journal of Magnetism and Magnetic Materials, 417, pp.6–10, (2016).
9. Hosny, N.M, "Synthesis, characterization and optical band gap of NiO nanoparticles derived from anthranilic acid precursors via a thermal decomposition route," Polyhedron, 30(3), pp.470–476, (2011).
10. Mateos, D., Valdez, B., Castillo, J.R., Nedev, N., Curiel, M., Perez, O., Arias, A. and Tiznado, H," Synthesis of high purity nickel oxide by a modified sol-gel method," Ceramics International, 45(9), pp.11403–11407, (2019).
11. Sheena, P. A., Priyanka, K. P., Sabu, N. A., Ganesh, S., & Varghese, T, "Effect of electron beam irradiation on the structure and optical properties of nickel oxide nanocubes," Bulletin of Materials Science, 38(4), 825-830, . (2015).
12. Y. Huang, "Sol-gel synthesis of NiO nanoparticles doped sodium borosilicate glass with third-order nonlinear optical properties", Journal of Alloys and Compounds, vol. 686, pp. 564-570, (2016).
13. Sery, A.A., Mohamed, W.A.A., Hammad, F.F., Khalil, M.M.H. and Farag, H.K, "Synthesis of pure and doped SnO2 and NiO nanoparticles and evaluation of their photocatalytic activity," Materials Chemistry and Physics, 275, p.125190, (2022).
14. M. Anitha, K. Saravanakumar, N. Anitha, and L. Amalraj, “Influence of a novel co-doping (Zn+ F) on the physical properties of nano structured (1 1 1) oriented CdO thin films applicable for window layer of solar cell” Appl. Surf. Sci., vol. 443, pp. 55–67, (2018).
15. Varshney, B., Siddiqui, M.J., Anwer, A.H., Khan, M.Z., Ahmed, F., Aljaafari, A., Hammud, H.H. and Azam, A, "Synthesis of mesoporous SnO2/NiO nanocomposite using modified sol–gel method and its electrochemical performance as electrode material for supercapacitors. Scientific Reports", 10(1), (2020).
16. Bahari Molla Mahaleh, Y., Sadrnezhaad, S.K. and Hosseini, D, "NiO Nanoparticles Synthesis by Chemical Precipitation and Effect of Applied Surfactant on Distribution of Particle Size," Journal of Nanomaterials, pp.1–4, (2008).

Proceeding of the Third International & the Fifth Scientific Conference of College of Science - Tikrit University
Int.3, Loc.5, Article ID:2022-P3-15

تأثير التشعيع على الخواص التركيبية والبصرية لجسيمات أكسيد النيكل النانوية المحضرة بطريقة (سول- جل).NiO

سندس احمد محمد ، جاسم محمد منصور ، عمر احمد موفق

قسم الفيزياء ، كلية العلوم ، جامعة ديالى، ديالى ، العراق

الملخص

تم في هذا البحث تصنيع اوكسيد النيكل النانوي NiO باستعمال تقنية Sol-gel بنسب مولارية مختلفة من نترات النيكل وحمض الستريك (P1,P2,P3)، وتلدينها عند (525 ˚C) ، ودراسة تأثير التشعيع على الخصائص التركيبية والبصرية لأوكسيد لجسيمات النيكل النانوية.

وفقًا لبيانات XRD ، تكون كل عينة متعددة التبلور ، مع هيكل مكعب مثل مستوى الاتجاه المفضل (200) ، وأن هذه النتائج تتوافق إلى حد كبير مع البطاقة القياسية (ICSD رقم 047-1049). بينت النتائج أن حجم الحبوب كان أقل مما كان عليه قبل التشعيع ، وهذا يعني أن التشعيع تسبب في زيادة تبلور الحبيبات وبالتالي انخفاض في حجم البلورات. أظهرت صور (FESEM) لجسيمات أكسيد النيكل النانوية قبل وبعد التشعيع أن الإشعاع يقلل من حجم الحبيبات باستثناء العينة (P3) ، مما يظهر عكس ذلك وهذه النتائج ، أظهرت النتائج البصرية أن عملية تشعيع أشعة جاما أدت إلى زيادة طفيفة في معامل الامتصاص والامتصاص ، وكذلك انخفاض في فجوة الطاقة الضوئية.